J|A|C|S
ARTICLES
Published on Web 03/12/2002

A First Transition Series Pseudotetrahedral Oxynitride Anion: Synthesis and Characterization of Ba_2VO_3N

Simon J. Clarke,*,† Paul R. Chalker,‡ Jasper Holman,§,⊥ Charles W. Michie,§ Matthieu Puyet,†,|| and Matthew J. Rosseinsky*,§

Contribution from the Inorganic Chemistry Laboratory, Department of Chemistry, University of Oxford, Oxford, OX1 3QR, U.K., Materials Science and Engineering, Department of Engineering, University of Liverpool, Liverpool, L69 7ZD, U.K., and Department of Chemistry, University of Liverpool, Liverpool, L69 7ZD, U.K.

Received October 3, 2001

Abstract: Ammonolysis of reactive oxide precursors affords the vanadium(V) phase Ba_2VO_3N that is shown by X-ray and neutron powder diffraction and Raman spectroscopy to contain pseudotetrahedral VO_3N^{4-} anions. This is the first example of such species for the first transition series metals.

Introduction

The interesting fundamental and technological properties of oxides and nitrides[1,2] have led to a recent upsurge of interest in the synthesis of mixed anion oxynitride[3] solids. The possibilities for property enhancement arising from the development of this synthetic chemistry are illustrated by the new oxynitride ATa$(O,N)_3$ (A = alkaline earth, lanthanide) red pigments.[4] A persistent problem in the preparation of oxynitrides is separation into monoanionic oxide and nitride phases, so the development of synthetic routes which avoid such problems is important. In this paper we demonstrate that reactive oxide precursors can be used to prepare oxynitrides, and use this chemistry to prepare Ba_2VO_3N. Although pseudotetrahedral oxide nitride anions are well-established for the second and third transition series (OsO_3N^-, ReO_3N^{2-}, WO_3N^{3-}),[5−7] the VO_3N^{4-} anion in Ba_2VO_3N is the first example of such a species for a first transition series metal.

Experimental Section

Synthesis. A precursor with a Ba:V ratio of 2:1 was prepared by dissolving separately 4.9629 g of $BaCO_3$ (25.150×10^{-3} mol) and 1.1436 g of V_2O_5 (6.288×10^{-3} mol) (both Alfa Puratronic 99.995%) in 250 cm^3 of 2 M nitric acid, with warming in the case of V_2O_5. The solutions were combined to give a pale orange solution to which 1 mol of citric acid per mole of metal ions (7.248 g, 37.726×10^{-3} mol) and 20 cm^3 of ethylene glycol were added, resulting in a blue solution. The solution was heated to boiling where it changed color to green. Evaporation produced a moist brown paste that was dried at 200 °C overnight, eventually leading to a dark green powder in which the only crystalline phase evident from X-ray powder diffraction was $Ba(NO_3)_2$.

$Ba_3V_2O_8$ was also prepared on the 5 g scale by this route with calcination to constant mass at 500−600 °C producing crystalline $Ba_3V_2O_8$. Alternatively, $Ba_3V_2O_8$ was prepared by reaction of V_2O_5 with $Ba(NO_3)_2$ at 800 °C for 24 h.

Precursor Ammonolysis. The reactive precursors were reacted under flowing anhydrous ammonia (BOC, 99.98%) in silica tubes as described previously.[8] The ammonia flow rate of 175 to 200 cm^3 min^{-1} was monitored with a Jencons MeTeRaTe flowmeter tube. A 0.5 g sample of Ba_2VO_3N for the neutron diffraction experiments was prepared by treating the citrate precursor at 900 °C for 15 h under flowing ammonia. Alternative routes to phase pure material are (a) reaction of a mixture of V_2O_5 with $Ba(NO_3)_2$, ground together under acetone and dried, with ammonia initially at 500 °C and then at 900 °C, or (b) reaction of BaO (prepared by thermal decomposition of $BaCO_3$) and $Ba_3V_2O_8$ for two periods of 15 h at 900 °C followed by 15 h at 1000 °C under flowing ammonia.

Manipulation of samples was performed under a helium atmosphere in an MBraun Labmaster drybox due to the air-sensitive nature of some of the possible intermediates.

Thermogravimetric Analysis. The identification of ammonolysis conditions which would afford the oxynitride phase was made using thermogravimetric analysis/mass spectrometry (TGA-MS) monitoring of the thermal behavior of the oxide precursors under a flow of 40% NH_3 in helium on a Seiko Instruments SII Exstar 6000 TGA instrument equipped with a Hiden Analytical HPR20 MS residual gas analyzer over the range $25 \leq T/°C \leq 1200$. The stability of Ba_2VO_3N under reducing and oxidizing conditions was studied by treatment with H_2 and O_2 over the range $25 \leq T/°C \leq 1000$.

* Address correspondence to these authors. E-mail: simon.clarke@chem.ox.ac.uk and m.j.rosseinsky@liv.ac.uk.
† University of Oxford.
‡ Materials Science and Engineering, Department of Engineering, University of Liverpool.
§ Department of Chemistry, University of Liverpool.
⊥ Current address: Materials Science Center, University of Groningen, Nijenborgh 4, 9747 AG, Groningen, The Netherlands.
|| Current address: Laboratoire de Physique des Materiaux (L.P.M), UMR CNRS-UHP-INPL 7556, Ecole Nationale Superieur des Mines de Nancy, Parc de Saurupt, 54042 Nancy Cedex, France.

(1) Brese, N. E.; O'Keeffe, M. *Struct. Bonding* **1992**, *79*, 309−340.
(2) Schnick, W. *Angew. Chem., Int. Ed. Engl.* **1993**, *32*, 806−818.
(3) Marchand, R.; Laurent, Y.; Guyader, J.; L'Haridon, P.; Verdier, P. *J. Eur. Ceramic Soc.* **1991**, *8*, 197−213.
(4) Jansen, M.; Letschert, H. P. *Nature* **2000**, *404*, 980−981.
(5) L'Haridon, P.; Pastuszak, R.; Laurent, Y. *J. Solid State Chem.* **1982**, *43*, 29−32.
(6) Laurent, Y.; Pastuszak, R.; L'Haridon, P.; Marchand, R. *Acta Crystallogr.* **1982**, *B38*, 914−916.
(7) Muller, A.; Krebs, B.; Holtje, W. *Spectrochim. Acta* **1967**, *23A*, 2753−2760.
(8) Clarke, S. J.; Michie, C. W.; Rosseinsky, M. J. *J. Solid State Chem.* **1999**, *146*, 399−405.

Vibrational Spectroscopy. Raman data were collected on samples sealed in capillaries using a fiber optic probe instrument based on a Renishaw Compact System 100 Spectrometer with an Ar^+ (514.531 nm) laser. IR data were collected on disks pressed from an approximately 10:1 mixture by mass of KBr and sample using a Bruker IFS 66v/s FTIR spectrometer

Diffraction Characterization. Laboratory X-ray powder diffraction data for phase identification and preliminary structural analysis were collected in transmission and reflection modes on a Stoe Stadi-P powder diffractometer with Cu $K\alpha_1$ radiation and linear position-sensitive detectors. Synchrotron X-ray powder diffraction data were collected on a portion of the neutron diffraction sample sealed under He in a 0.5 mm capillary on station 9.1 of the Synchrotron Radiation Source at Daresbury Laboratory ($\lambda = 0.9980$ Å).

Neutron powder diffraction data were collected at room temperature on the POLARIS time-of-flight neutron powder diffractometer, at the ISIS Facility, Rutherford Appleton Laboratory. The sample was contained in a 6 mm diameter vanadium can. Rietveld refinement was performed with the GSAS software,[9] with the final structural model derived from simultaneous refinement against all three detector banks of neutron data (35°, 90°, and 145° covering a range $0.5 \leq d/\text{Å} \leq 6.5$) and the synchrotron X-ray data. The following neutron scattering lengths were used: Ba, 5.25 fm; V, −0.38 fm; O, 5.805 fm; N, 9.36 fm.

Chemical Analysis. CHN combustion analysis was used initially to determine the nitrogen and hydrogen content of samples, using a Carlo Erber Strumentazione 1106 CHN analyzer. ICP (Inductively Coupled Plasma emission spectroscopy) elemental analysis for barium and vanadium was performed using a Thermo Elemental Atomscan 16 instrument.

Magnetic Measurements. Data were collected on a Quantum Design MPMS SQUID magnetometer over the range $2 \leq T/\text{K} \leq 20$ and at 300 K.

Results

$Ba_3V_2O_8$ prepared by the citrate gel route reacted with ammonia at 750 °C to afford Ba_2VO_3N and VN. $Ba_3V_2O_8$ derived from the conproportionation of $Ba(NO_3)_2$ and V_2O_5 reacted incompletely at 900 °C to produce Ba_2VO_3N together with unreacted $Ba_3V_2O_8$, although previous reports[10,11] suggest that $Ba_3V_2O_8$ is completely resistant to nitridation by ammonolysis. Ba_2VO_3N was identified by structural analogy with β-Ba_2VO_4[12] and β-Ca_2SiO_4 together with the analyzed N content, but the $Ba_3V_2O_8$ phase is clearly an unsuitable precursor due to its composition. In the absence of well-characterized oxides with a 2:1 Ba:V ratio, we used reactive oxide precursors derived from decomposition of citrate gels or metal nitrate/oxide mixtures with the correct composition.

The synthesis of Ba_2VO_3N requires precise control of the competing reactions which occur when Ba_2VO_x precursors are ammonolyzed. The reaction must be run so as to avoid the formation of Ba_3VO_5, which appears stable under the ammonolysis conditions. Preliminary experiments revealed that the formation of VN and Ba_3VO_5 could be avoided by using two reactive oxide precursors with a Ba:V ratio of 2:1, derived either from a citrate gel or by intimately mixing $Ba(NO_3)_2$ with V_2O_5. The ammonolysis of these precursors produced complex reaction products, so the conditions required to isolate the oxynitride phase were identified by monitoring the ammonolysis reaction of the precursor by TGA under a dilute flow of NH_3 in He up to 1200 °C. This (Figure 1) revealed a complex series of reaction steps leading to a mixture of Ba_2VO_3N, $Ba_3V_2O_8$, and BaO via several intermediate plateaux, including the $Ba_4V_2O_9$ composition (600 °C, mass 64.6%, Figure 1b). Ba_2VO_3N is visible in X-ray patterns taken both at the 63.6% mass plateau at 975 °C (where it is the minor component, and $Ba_3V_2O_8$ predominates) and in the final post-1200 °C product, where it is the major component, suggesting that this temperature range was appropriate for its synthesis.

The phases identified at the plateaux (Figure 1b) in the TGA experiment were then confirmed by synthesis in bulk with pure ammonia at 500 °C ($Ba_4V_2O_9$ + BaO, Figure 2a) and 700 °C ($Ba_3V_2O_8$ + BaO + Ba_2VO_3N, Figure 2b). Synthesis under flowing ammonia at 900 °C yielded phase-pure Ba_2VO_3N in the case of both precursors (Figure 2c); the higher ammonia fugacity of the large-scale synthesis leads to pure Ba_2VO_3N rather than a multiphase mixture, and at a lower final temperature. Two treatments of 15 h with intermediate regrinding were required to afford a homogeneous gray-green product. After the first treatment, material at the top of the boat appeared yellow-green in contrast to the gray material beneath. The Ba:V ratio was 2.2(1) according to ICP. The calculated N content of 3.61% agrees well with 3.55% observed for Ba_2VO_3N produced by ammonolysis of BaO and $Ba_3V_2O_8$, though the sample used in neutron diffraction has a higher nitrogen content of 4.28%. The H content was found to be zero. The concentration of VN in the material was determined to be less than 0.1% according to the superconducting volume fraction determined by magnetization measurements. Above the transition temperature of VN the susceptibility of 2.6×10^{-4} emu mol^{-1} is temperature independent, indicating the absence of V(IV).

Ba_2VO_3N is stable for days but not months on standing in laboratory air. Oxidation leads to $Ba_3V_2O_8$ and BaO ($BaCO_3$ after exposure to air), while the products of treatment with H_2 are $Ba_3V_2O_8$ and Ba_2VO_4 (after exposure to air).

Analysis of the X-ray powder diffraction pattern of Ba_2VO_3N with the TREOR[13] autoindexing software led to the identification of an orthorhombic cell of dimensions $5.94 \times 7.706 \times 10.515$ Å^3, suggesting a strong structural analogy with monoclinic Ba_2VO_4. Refinement of lab X-ray powder data proceeded satisfactorily in either the orthorhombic *Pnma* symmetry α-K_2SO_4[14] structure or the monoclinic β-Ba_2VO_4 structure.[12] However, analysis of the higher resolution synchrotron X-ray data revealed that the *Pnma* model was correct, although correction for significant anisotropic peak broadening[15] was required for a truly quantitative fit. The Ba:V ratio refined to 2.05(3) and was fixed at 2 in subsequent analyses. Precise location of the anions in the presence of Ba requires the use of neutron data, while the refinement of the V position is not possible with neutron data alone due to the near-zero scattering length of vanadium. Combined analysis of the X-ray and neutron histograms is therefore essential for a precise structural analysis of this material. Refinement with isotropic temperature factors proceeded smoothly to $\chi^2 = 2.1$ but with significant features in the difference Fourier (ΔF) map in the environment of the VO_3N^{4-} unit. Refinement with anisotropic temperature factors

(9) Larson, A. C.; von Dreele, R. B. *General Structure Analysis System*; Los Alamos National Laboratory, 1994.
(10) Subramanya Herle, P.; Hegde, M. S.; Subbanna, G. N. *J. Mater. Chem.* **1997**, *7*, 2121−2125.
(11) Li, H.-Z.; Liu, L.-M.; Reis, K. P.; Jacobson, A. J. *J. Alloys Compd.* **1994**, *203*, 181−187.
(12) Liu, G.; Greedan, J. E. *J. Solid State Chem.* **1993**, *103*, 228−239.
(13) Werner, P.-E.; Eriksson, L.; Westdahl, M. *J. Appl. Crystallogr* **1985**, *18*, 367−370.
(14) Catti, M.; Gazzoni, G.; Ivaldi, G. *Acta Crystallogr. C* **1983**, *39*, 29−34.
(15) Stephens, P. *J. Appl. Crystallogr*. **1999**, *32*, 281−289.

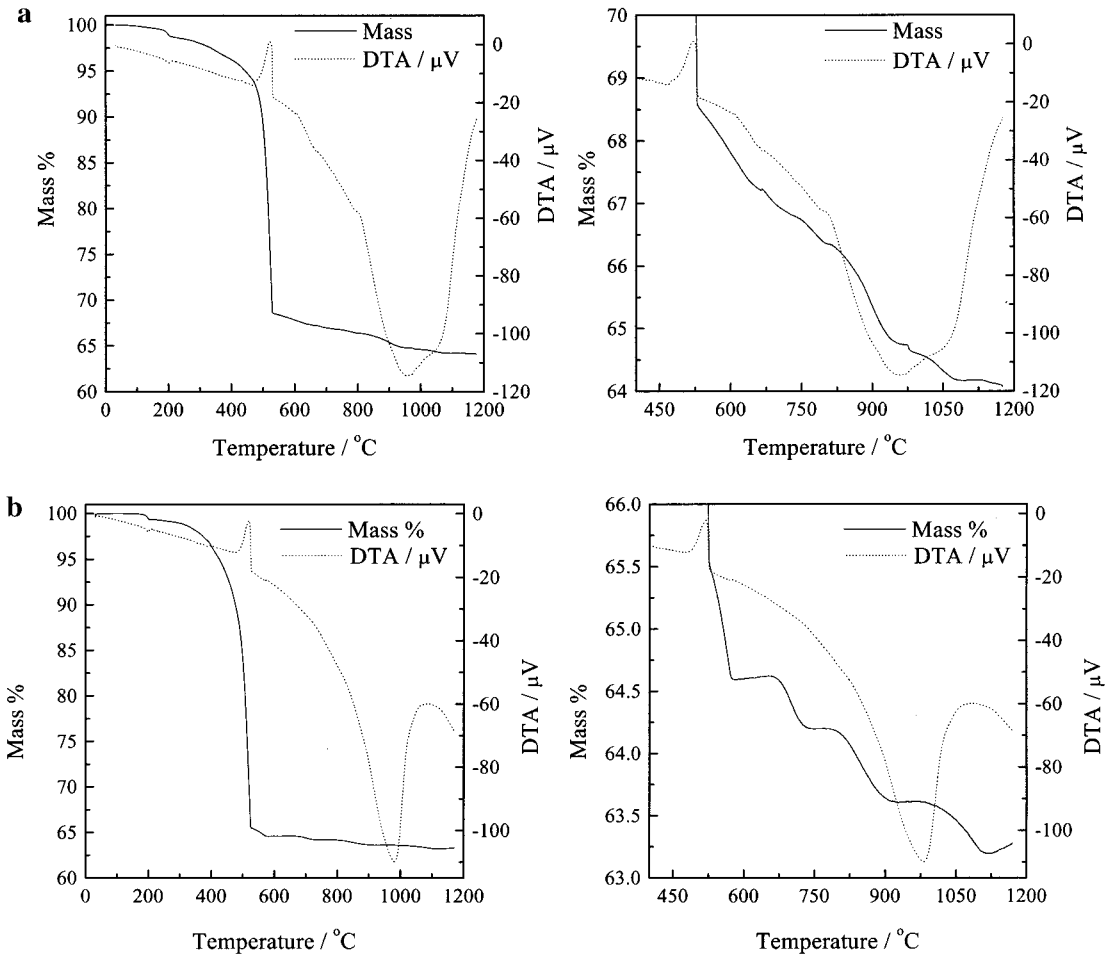

Figure 1. Thermogravimetric analysis of (a) Ba_2VO_x citrate gel precusor and (b) $2Ba(NO_3)_2 + V_2O_5$ under a flow of 400 cm^3min^{-1} of 40% NH_3 in He. The right panel in each case focuses on the temperature region in which the competing reactions occur. The plateau in part b at 64.6% corresponds to the formation of $Ba_4V_2O_9$ (expected mass 64.8%) and the total mass of 63.2% compares with 63.17% expected for the formation of Ba_2VO_3N.

reduced χ^2 significantly to 1.52 and removed all the structure from the ΔF map (the highest ΔF peak was 0.7% of the F_{obs} maximum and refined to zero occupancy when incorporated into the model). There was no evidence for different ordered V−O and V−N bond lengths when the positional parameters of the O and N anions occupying the same site were refined separately. The refinements against the synchrotron and highest resolution neutron data are given in Figure 3 (the refinements of the other two neutron datasets are given in Figure S1). The refined structure and the VO_3N^{4-} unit are shown in Figure 4. The refined positional parameters are given in Table 1, the displacement parameters in Table 2, and the agreement indices in Table 3. The occupancy of each anion site was freely refined between O and N with the total occupancy fixed at 100%, yielding a refined composition of $Ba_2VO_{2.97(3)}N_{1.03(3)}$. An impurity of 2.7(1) mol % VN is present.

The mean V−O/N bond length within the VO_3N^{4-} unit is 1.73(1) Å and the mean O/N−V−O/N angle is 109(2)°. (Table 4) The mean bond length is less than 1.76(3) Å found for the $V^{IV}O_4^{4-}$ tetrahedron in Ba_2VO_4[12] and slightly longer than 1.71(1) Å in $V^{V}O_4^{3-}$ in $Ba_3V_2O_8$[16] and $Sr_3V_2O_8$.[17] The closest intertetrahedron V−O/N contact of 3.86 Å demonstrates that the VO_3N^{4-} anions are isolated from each other. The *Pnma*

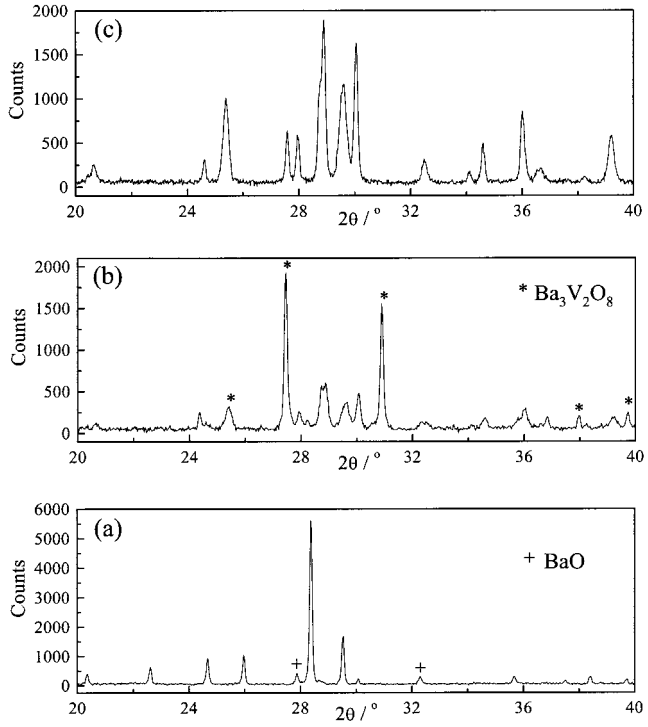

Figure 2. X-ray powder diffraction data from $2Ba(NO_3)_2 + V_2O_5$ after reaction with NH_3 at (a) 500, (b) 700, and (c) 900 °C.

(16) Liu, G.; Greedan, J. E. *J. Solid State Chem.* **1994**, *110*, 274−289.
(17) Carrillo-Cabrera, W.; von Schnering, H. G. *Z. Kristallogr.* **1993**, *205*, 271−276.

Table 1. Positional Parameters and Fractional Occupancies from the Combined X-ray and Neutron Refinement of Ba_2VO_3N at 293 K[a]

	x	*y*	*z*	$U_i/U_e \times 100$ (Å^2)	Wyckoff position	fractional occupancy
Ba(1)	0.15723(8)	0.75	0.08036(8)	1.20*	4c	1
Ba(2)	0.01054(8)	0.25	0.30749(6)	0.63*	4c	1
V	0.2270(2)	0.75	0.4206(3)	0.51(5)	4c	1
O/N(1)	0.0049(1)	0.75	0.4168(1)	2.08*	4c	0.676(8)
O/N(2)	0.3061(1)	0.75	0.57428(9)	1.57*	4c	0.558(8)
O/N(3)	0.3092(1)	0.5090(2)	0.34784(6)	1.63*	8d	0.866(6)

[a] For sites occupied by the O and N anions in a disordered manner, the O occupancy is quoted. The displacement parameters marked by asterisks are isotropic equivalents derived from the anisotropic values listed in Table 2. *Pnma*, $a = 7.70736(4)$ Å, $b = 5.92871(3)$ Å, $c = 10.50584(5)$ Å, $V = 480.061(4)$ Å^3

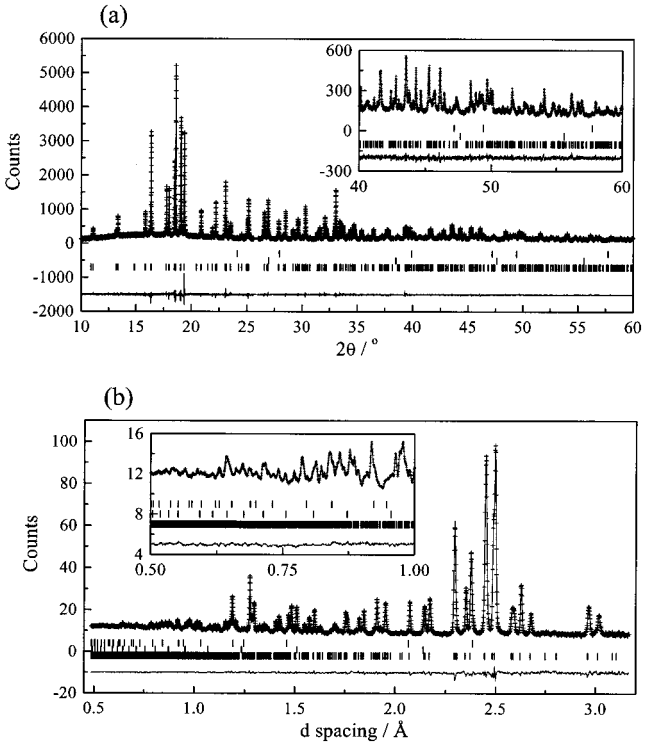

Figure 3. Rietveld refinement of (a) synchrotron X-ray ($\lambda = 0.9980$ Å) and (b) neutron time-of-flight (backscattering detectors $2\theta = 145°$) diffraction patterns of Ba_2VO_3N. The observed data are shown as points, the calculated model is the solid line, and the difference curve is shown below. Markers indicate the position of the Bragg reflections from Ba_2VO_3N (bottom), VN (top), and V (middle).

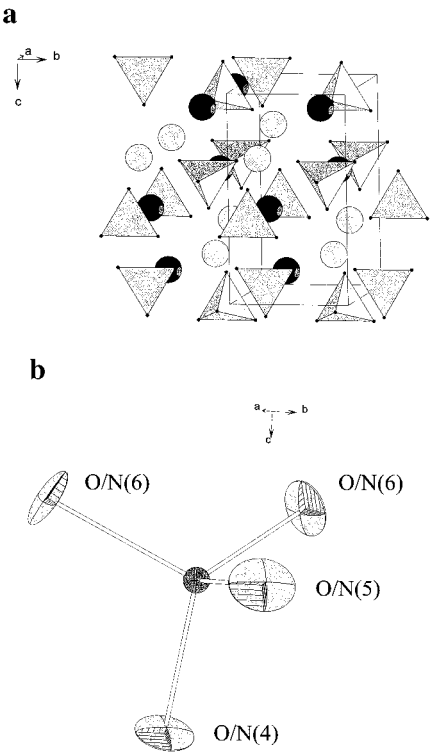

Figure 4. (a) Polyhedral representation of the structure of Ba_2VO_3N. The Ba(1) cations are the darker spheres, with the Ba(2) cations having lighter shading. (b) Thermal ellipsoids (70% probability) of the VO_3N^{4-} anion.

Table 2. Anisotropic Displacement Parameters (Å^2) for Ba_2VO_3N at 293 K

	U_{11}	U_{22}	U_{33}	U_{12}	U_{13}	U_{23}
Ba(1)	0.68(3)	1.02(4)	1.89(4)	0	0.32(3)	0
Ba(2)	0.27(3)	1.10(4)	0.52(3)	0	0.15(3)	0
O/N(1)	0.55(4)	3.66(8)	2.03(6)	0	−0.55(5)	0
O/N(2)	1.11(5)	2.78(6)	0.83(5)	0	−0.77(4)	0
O/N(3)	1.58(3)	1.05(4)	2.24(4)	0.17(4)	0.77(4)	−0.93(3)

Table 3. Goodness-of-Fit Parameters from Combined X-ray and Neutron Refinement of Ba_2VO_3N at 293 K[a]

	N	R_{wp}/%	R_E/%	R_F^2/%
neutrons, 145° detectors	3746	1.11	0.84	5.06
neutrons, 90° detectors	4268	1.63	1.23	7.29
neutrons, 35° detectors	4430	2.60	2.72	4.24
X-rays	9888	5.65	4.40	3.67

[a] $\chi^2 = 1.55$ for 22 332 observations.

symmetry yields three distinct anion sites whose occupancy demonstrates partial O/N order and orientational disorder of the VO_3N^{4-} anion. The longest V−O/N bond of 1.739(2) Å is to the O/N(3) site, which is 86.6(6)% occupied by O, consistent with a charge distribution in the anion with V═N$^-$ and V−O$^-$ bonding predominating. The O/N(1) (V−O/N 1.712(2) Å, 67.6(8)% O) and O/N(2) (V−O/N 1.725(4) Å, 55.8(8)% O) sites have similar O/N occupancies and bond distances: the longer V−O/N bond at the more N-rich site 2 is surprising but needs to be considered in the light of the larger number of close contacts between this site and the barium cations.

The two Ba environments are ten and nine coordinate (Table 4). The nine-coordinate environment of Ba(2) consists of six shorter distances of less than 2.83 Å to anions which describe a heavily distorted octahedron that is capped on three adjacent faces by more distant anions (Figure 5a). These capped octahedra share faces along the [100] direction to form chains which are linked by the capping anions via the VO_3N^{4-} units to six neighboring chains: the capping O/N(1) anions have the shortest V−O/N distance, which accounts for their more distant coordination to Ba(2) (Figure 5b).

Ba_2VO_3N adopts the α′ orthorhombic modification of the K_2SO_4 structure, which is derived from the hexagonal high-temperature aristotype. The *a* axis is the pseudo-6-fold axis,

Table 4. Bond Lengths (Å) and Angles (deg) in (a) the VO_3N^{4-} Anion and (b) Around the Two Barium Sites in Ba_2VO_3N at 293 K

(a) VO_3N^{4-} Anion	
V−O/N(1)	1.713(2)
V−O/N(2)	1.726(3)
V−O/N(3) (×2)	1.740(2)
O/N(1)−V−O/N(2)	112.0 (1)
O/N(1)−V−O/N(3) (×2)	110.72(9)
O/N(2)−V−O/N(3) (×2)	106.41(9)
O/N(3)−V−O/N(3)	110.4 (1)
(b) Around the Two Barium Sites in Ba_2VO_3N	
Ba1−O/N(1)	2.679(1)
Ba1−O/N(3) (×2)	2.897(1)
Ba1−O/N(2) (×2)	2.979(1)
Ba1−O/N(3) (×2)	3.131(1)
Ba1−O/N(2)	3.157(1)
Ba1−O/N(3) (×2)	3.363(1)
Ba2−O/N(3) (×2)	2.726(1)
Ba2−O/N(2)	2.738(1)
Ba2−O/N(3) (×2)	2.800(1)
Ba2−O/N(2)	2.829(1)
Ba2−O/N(1)	2.899(1)
Ba2−O/N(1) (×2)	3.1793(5)

Table 5. Raman Observed Modes (cm^{-1}) in Ba_2VO_3N and $Ba_3V_2O_8$[a]

	Ba_2VO_3N	$Ba_3V_2O_8$
ν_1	927, 913, 891	835
ν_3	736, 762	778
ν_4	382	379, 416
ν_2	322	328

[a] Only the ν_1 mode of Ba_2VO_3N has been deconvolved.

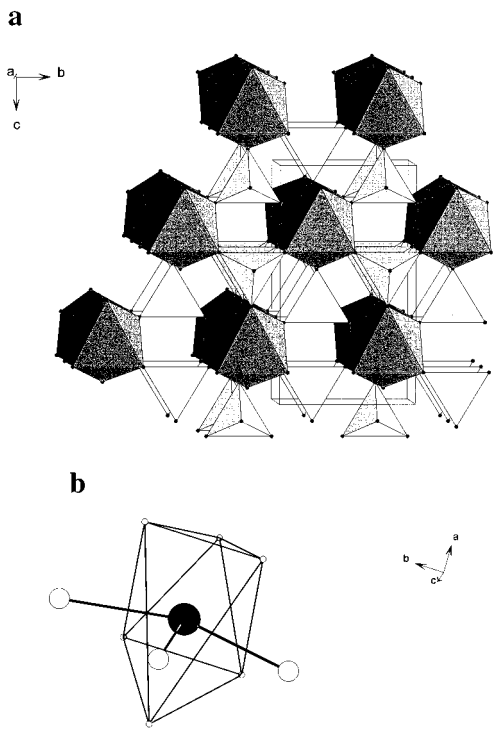

Figure 5. (a) The Ba(2) units are distorted octahedral face-sharing chains cross-linked by the O/N(4) anions which (b) cap three adjacent faces.

and the shortest V−O/N(1) distances are aligned parallel and antiparallel to this direction in neighboring chains of VO_3N^{4-} units separated by Ba(1) cations (Figure 4b). The Ba(1) polyhedron has pseudo-6-fold symmetry when viewed along [100], which is the direction of the shortest Ba(1)−O/N(1)

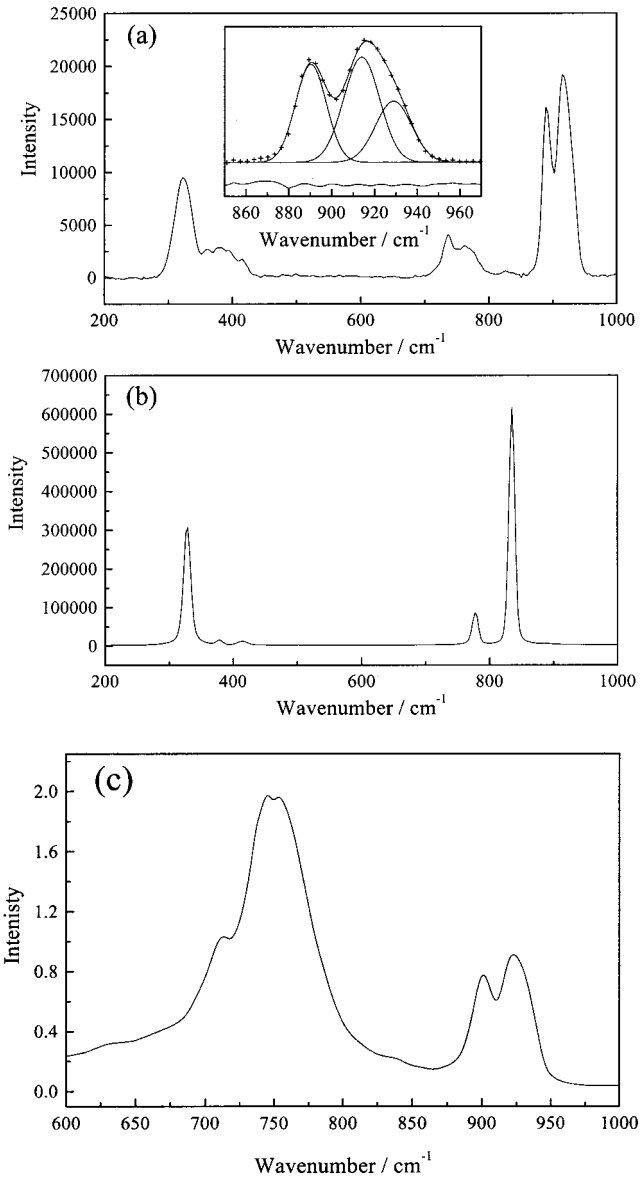

Figure 6. Raman spectra of (a) Ba_2VO_3N and (b) $Ba_3V_2O_8$. The inset in part a shows how the ν_1 mode can be fitted as three distinct modes. (c) Infrared spectrum of Ba_2VO_3N showing the expected reversal in relative intensity of the ν_1 and ν_3 stretching modes.

contact, with the 10-fold coordination consisting of three anions on the opposite side of Ba(1) to the shortest contact with six almost coplanar Ba-anion bonds. These contacts arise because the $Ba(1)(O,N)_{10}$ polyhedron has five VO_3N^{4-} units as near neighbors: the six anions forming the hexagonal ring arise from three edge-sharing anion pairs from three (100) plane VO_3N^{4-} neighbors, and the three anions opposite the short Ba(1)−O/N(1) contact are a triangular face of the fifth VO_3N^{4-} neighbor. The three hexagon edges not shared with VO_3N^{4-} units are shared with other $Ba(1)(O,N)_{10}$ polyhedra. The shorter mean distances between Ba(2) and the anions can be correlated with the smaller displacement parameter at this site.

The observation of Raman active modes with frequencies of higher than 900 cm^{-1} clearly indicates the formation of V═N bonds as no modes are observed at above 840 cm^{-1} for VO_4^{3-} units. The A_1 and T_2 stretching modes of a tetrahedron split into a high-frequency ν_1 A′ (predominantly MN) and lower frequency ν_3 (2A′ + A″, predominantly MO_3) modes in MO_3N

species with m (C_s) symmetry.[18] Comparison of the Raman spectra with the $V^vO_4^{3-}$ units in $Ba_3V_2O_8$ (Figure 6a) reveals that the ν_3 modes occur at similar frequency in both $Ba_3V_2O_8$ and Ba_2VO_3N but are considerably broadened in the oxynitride anion, while the ν_1 mode is shifted to higher frequency. The local m symmetry of the anion means that it must adopt three inequivalent orientations because each of the three crystallographically distinct anion sites has nonzero O and N occupancies. This is expected to lead to one A' mode for each orientation, and these are observed at 927, 913, and 891 cm^{-1} (see the inset to Figure 6a). The ν_1/ν_3 ratio is higher than in VO_4^{3-} (1.21 vs 1.04) in accord with expectation based on increased anionic charge.[18] The infrared spectrum (Figure 6b) shows that as expected[19] the relative intensities of the ν_1 and ν_3 modes are reversed. Fitting of the infrared spectrum yields three ν_1 A' modes at 933, 921, and 900 cm^{-1}.

Discussion

The VO_3N^{4-} anion is the first example of an isolated MO_3N species for the first transition series. The absence of other examples is surprising, as the nitride anion is a strong π-donor well-suited to interacting with d^0 metal centers. Many oxynitride perovskites with six-coordinate first-row transition metals are known, and tetrahedral environments for these metals are quite common for ternary nitrides of the first-row transition metals especially when the ratio of electropositive (e.g. alkaline earth) metal to transition metal is large (e.g. >2:1). Examples include A_2VN_3 (A = Sr, Ba; V^V),[20] $Ba_{10}Ti_4N_{12}$ (Ti^{IV}),[21] and Ba_5CrN_5 (Cr^V).[22] In these cases, as in the case considered here, the high coordination number and low electronegativity of the alkaline earth stabilizes the high oxidation state and four-coordination of the transition metal. Given that the early transition metals commonly exhibit four-coordination in both oxides and nitrides it is likely that appropriate synthetic routes to the isolation of other first series MO_3N^{m-} anions have yet to be identified. The reaction sequence leading to Ba_2VO_3N is complex: although $Ba_3V_2O_8$ is reported to be stable under NH_3, it is formed here and then reacts with BaO or Ba-rich vanadium oxide phases to afford Ba_2VO_3N, indicating that the higher Ba:V ratio is important in stabilizing the tetrahedral oxynitride anion. The previous reports[10,11] that $Ba_3V_2O_8$ is stable at 900 °C under NH_3 contrast with the formation of Ba_2VO_3N and VN from citrate gel derived $Ba_3V_2O_8$ reported here and suggest that the kinetic advantages of small particle oxide precursors can be crucial in yielding new oxynitrides in ammonolysis reactions. Reinvestigation of the reactivity of other ternary oxides thought unreactive to ammonia in the light of these results is warranted.

Acknowledgment. We thank EPSRC for support under GR/L60067. We thank Dr. M. A. Roberts, Dr. R. M. Ibberson, and Dr. R. I. Smith for assistance with collection of Synchrotron X-ray and neutron diffraction data, Dr. R. J. Nichols (University of Liverpool) for assistance with collection of infrared spectroscopy data, and Dr. J. B. Claridge (University of Liverpool) and Professor R. G. Denning (University of Oxford) for wide-ranging and helpful discussion.

Supporting Information Available: Figure showing the Rietveld refinement of neutron prowder diffraction from Ba_2VO_3N collected on the POLARIS instrument (PDF). This material is available free of charge via the Internet at http://pubs.acs.org.

JA0122896

(18) Nakamoto, K. *Infrared and Raman spectra of inorganic and coordination compounds*; Wiley-Interscience: New York, 1986.
(19) Gonzalez-Vilchez, F.; Griffith, W. P. *J. Chem. Soc., Dalton Trans.* **1972**, 1416−1421.
(20) Gregory, D. H.; Barker, M. G.; Edwards, P. P.; Siddons, D. J. *Inorg. Chem.* **1995**, *34*, 3912−3916.
(21) Seeger, O.; Strähle, J. *Z. Anorg. Allg. Chem.* **1995**, *621*, 761−764.
(22) Tennstedt, A.; Kniep, R.; Hüber, M.; Haase, W. *Z. Anorg. Allg. Chem.* **1995**, *621*, 511−515.